applied sciences

MDPI

Article

Methodology for the Prediction of the Thermal Conductivity of Concrete by Using Neural Networks

Ana Carolina Rosa [1,2], Youssef Elomari [2], Alejandro Calderón [3], Carles Mateu [4], Assed Haddad [1] and Dieter Boer [2,*]

[1] Environmental Engineering Program, Federal University of Rio de Janeiro, Rio de Janeiro 21941-901, Brazil; carolinarosa@poli.ufrj.br (A.C.R.); assed@poli.ufrj.br (A.H.)
[2] Department of Mechanical Engineering, University Rovira i Virgili, Av. Països Catalans 26, 43007 Tarragona, Spain; youssef.elomari@urv.cat
[3] Department of Materials Science and Physical Chemistry, Universitat de Barcelona, Martí i Franquès 1-11, 08028 Barcelona, Spain; acalderon@ub.edu
[4] Department of Computer Science and Industrial Engineering, University of Lleida, 25003 Lleida, Spain; carles.mateu@udl.cat
* Correspondence: dieter.boer@urv.cat

Abstract: The energy consumption of buildings presents a significant concern, which has led to a demand for materials with better thermal performance. Thermal conductivity (TC), among the most relevant thermal properties, is essential to address this demand. This study introduces a methodology integrating a Multilayer Perceptron (MLP) and a Generative Adversarial Network (GAN) to predict the TC of concrete based on its mass composition and density. Three scenarios using experimental data from published papers and synthetic data are compared and reveal the model's outstanding performance across training, validation, and test datasets. Notably, the MLP trained on the GAN-augmented dataset outperforms the one with the real dataset, demonstrating remarkable consistency between the model's predictions and the actual values. Achieving an RMSE of 0.0244 and an R^2 of 0.9975, these outcomes can offer precise quantitative information and advance energy-efficient materials.

Keywords: artificial neural networks; MLP; GAN; concrete; thermal conductivity

Citation: Rosa, A.C.; Elomari, Y.; Calderón, A.; Mateu, C.; Haddad, A.; Boer, D. Methodology for the Prediction of the Thermal Conductivity of Concrete by Using Neural Networks. *Appl. Sci.* **2024**, *14*, 7598. https://doi.org/10.3390/app14177598

Academic Editors: Daniel Ferrández Vega and Alexander Martín Garín

Received: 29 July 2024
Revised: 20 August 2024
Accepted: 20 August 2024
Published: 28 August 2024

1. Introduction

Driven by a growing sustainability awareness, energy efficiency is a topic that researchers are addressing more and more. As in other areas, concerns about energy efficiency solutions for buildings have largely increased. For this reason, the demand for the development of materials to improve thermal performance in buildings has increased. An appropriate design and material selection can lead to more environmentally responsible and economically sustainable construction practices. Using materials for better thermal efficiency can preserve indoor thermal comfort despite fluctuations in outdoor environment conditions and reduce energy consumption [1].

In the building design phase, vast possibilities for methods and materials exist to guarantee an adequate combination to achieve an energy-efficient building. Two types of methods can be used to improve the energy efficiency of a building: active methods and passive methods. The first type of method incorporates energy-efficient technologies to use or produce energy in the building, such as heat pumps and solar photovoltaic panels. The second type of method uses some countermeasures to reduce the thermal transmittance of the structure and enhance this efficiency using materials with low thermal conductivity. For instance, concrete can be used as part of the building envelope to improve energy efficiency [2]. It is the most used and stands out the most among the different building materials due to its unique features. Besides its resistance, durability, and low cost, its

inherent thermal mass attracts decision-makers. It allows heat to be absorbed, stored, and gradually released, stabilizing indoor temperatures and reducing unnecessary heating or cooling [3]. However, as concrete is a composite material of cement, water, fine aggregate, and coarse aggregate, its composition presents a wide variety, leading its properties to undergo significant variations [4]. Adjusting these constituents and their quantities allows the properties of both fresh and hardened states to be tailored to achieve the required design specifications. Thus, a specific property can be increased or decreased by changing the mass composition or including different constituents in a concrete mixture.

Thermal conductivity is one fundamental property affecting a material's energy efficiency, which measures how well a material conducts heat. Regarding the effect of heat transfer in a building, materials with low thermal conductivity value are used as insulation. They reduce the heat transfer between theinside and outside of the building, which maintains comfortable temperatures and reduces the energy consumption of heating and cooling systems. Factors influencing concrete's thermal conductivity include the constituents' type and weight, such as fine and coarse aggregates, supplemental cementitious materials (SCMs), and fibers [5]. Since a concrete composition contains 50–70% aggregates, their mineralogy and volume in the mixture have the most effect on the thermal conductivity of concrete [6].

Accurately predicting the thermal conductivity of concrete becomes vital to improving buildings' energy efficiency. A prediction model can help avoid many time-consuming experiments in the design and material selection phases. In recent years, machine learning (ML) models have been used to predict some properties of concrete, such as compressive strength [7], tensile strength [8], modulus of elasticity [9], flexural strength [10], slump [11], chloride penetration [12], carbonation depth [13], and surface chloride concentration [14]. Although many researchers have used ML, there is a limitation in studies developing prediction models of the thermal properties of concrete [15]. Among the machine learning-based models, the artificial neural network (ANN) is one of the most employed ones to solve complex problems and has applications in many fields [16–18]. The importance of ANNs lies in their ability to learn and make decisions based on data, which makes them highly valuable in different areas. An ANN is composed of a set of networks of interconnected nodes, which work together to learn complex relationships between a group of inputs and outputs. This makes them well suited for predicting some values based on a variety of parameters. In this way, ANNs can be used to solve problems that conventional or other computational methods have difficulties with [19]. ANNs provide an alternative method for predicting concrete properties that is faster, cheaper, and more accurate than traditional methods.

One of the drawbacks typically encountered when developing an ANN is a limited dataset, and effectively training an ANN requires a massive amount of data. When this problem arises, an alternative that has been emerging is the use of a Generative Adversarial Network (GAN). GANs were introduced by Goodfellow et al. [20] and became a revolutionary development in the world of generative modeling. They have different applications, such as image generation, super-resolution imaging, style transfer, and data augmentation. Regarding tabular data, they can create synthetic data to expand real datasets and prevent over-fitting in such data-limited situations, helping to improve the training of an ML model. Although GANs started with image generation, some authors have already used this technique to create tabular data and obtain satisfactory results. Since the introduction of GANs, several algorithms to model tabular data have been used, such as a Conditional Tabular GAN (CTGAN) [21], TabGAN, and CopulaGAN [22]. Although many researchers have attempted to use ANNs to predict different properties of concrete, only a few works are progressing on models to determine the thermal properties. Additionally, the papers do not have a generalist model focusing on different types of concrete, including its many constituents.

This work intends to fill this gap, and the novelty is the development of a methodology using an ANN model integrated with a data augmentation model to predict the thermal

properties of concrete containing different types of materials such as slag, lightweight and recycled aggregates, fibers, and others. For this methodology, a Multilayer Perceptron (MLP) model to predict thermal conductivity and a Copula GAN model to improve the tabular data from published papers will be developed based on the constituents' composition and the concrete's density.

The rest of the paper is organized as follows. Section 2 provides an overview of the ANN used to predict the properties of concrete. Next, Section 3 describes the methodology adopted for this work. Section 4 evaluates the results using a case study and discusses the main findings. Finally, the final section contains concluding remarks on the general findings.

2. Overview of Neural Networks

Over the years, ANNs have been applied to predict different properties of concrete due to their ability to model complex non-linear relationships. Regarding the property predictions, the mechanical properties are the most evaluated, with compressive strength being the most investigated in different machine learning models. Yeh was one of the pioneers applying an ANN to predict the properties of concrete and developed some models to predict compressive strength and slump [23,24]. Kandiri et al. estimated compressive strength using a hybrid model of an ANN and the salp swarm algorithm [25]. Abellán-García trained an MLP model to forecast the compressive strength for a given ultra-high-performance concrete mixture design [26]. Besides this, another work also developed an ANN with a feedforward backpropagation algorithm to predict slump flow and compressive strength while incorporating silica fume, limestone powder, recycled glass powder, and fluid catalytic cracking residue [27].

Although many studies are developing new models to predict the properties of concrete, only a few papers have investigated thermal conductivity or other thermal properties. Fidan et al. [28] trained different structures of an ANN model to predict thermal conductivity through five parameters—density, compressive strength, tensile strength, porosity, and ultrasonic pulse velocity. The best solution performance was achieved with a neural network with three layers and the following neuron sequence of 5, 25, and 1 in each layer. Sargam et al. [6] evaluated nine machine learning models, and MLP showed the highest prediction accuracy using the maxout activation function and three hidden layers, each containing 100 neurons. Kurpińska et al. [29] also investigated the influence of varying the number of neurons in the hidden layer to forecast the thermal conductivity of lightweight concrete. The model presented a sigmoid function and a structure with four layers: an input layer with two neurons, a first hidden layer varying from 2 to 12, a second hidden layer ranging from 2 to 17, and an output with one neuron. Kursuncu et al. [30] used an ANN and ANOVA to investigate the effect of partial replacement with waste marble powder and rice husk ash instead of fine aggregate and cement into foam concrete. The results indicated the ANN as the most adequate to estimate the thermal conductivity. Gence et al. [31] compared two neural networks, a radial basis neural network and an MLP, to predict the thermal conductivity of concrete with vermiculite and concluded that the former had greater accuracy.

Different types of ANNs have been successfully applied to predict the thermal conductivity of concrete. Table 1 compares some studies using distinct architectures of ANNs, and indicates that most models employ the backpropagation algorithm and do not have an extensive database.

Table 1. Comparative studies of different ANN-based methods to predict thermal conductivity.

Reference	ML Method	Concrete	Number of Inputs	Number of Hidden Layers	Neurons of Hidden Layers	Number of Outputs	Number of Datasets	Activation Function	Evaluation Criteria
Sargam et al. [6]	MLP	Concrete containing modern constituent materials	3, 5, 6, 8, 9, 10,13	3	100 100 100	1	213	Maxout	MAE
Fidan et al. [28]	ANN	Concrete	5	1	5, 10, 15, 20, 25	1	132	Tangent sigmoid	MAE, MAPE, RMSE, R^2
Kurpińska et al. [29]	Backpropagation NN	Lightweight concrete	2	2	2–12 2–17	1	15	Sigmoid	MSE
Kursuncu et al. [30]	ANN	Foam concrete	-	-	-	1	18	Sigmoid	R
Gencel et al. [31]	Radial basis NN/MLP	Concrete with vermiculite	5	1	3	1	20	Non-linear	RMSE, MSE, R
Lee et al. [32]	Backpropagation NN	Concrete	11	2	20 20	1	152	Sigmoid/linear	MSE, R
Ozel and Topsakal [33]	Backpropagation NN	Construction materials	2	1	1	1	110	-	RMSE, R^2
Ipek et al. [34]	Backpropagation NN	Rubberized concrete	5	1	2–20	1	127	Tangent hyperbolic	R^2, MAPE, MSE

Besides this brief literature overview, a general bibliometric analysis was performed to identify the most relevant and influential literature in predicting the properties of concrete using machine learning. This approach enables the identification of critical research gaps and areas for future investigation. To proceed with this analysis, VOSviewer software 1.6.19 [35] was used. It visually represents the research and supports researchers in finding insights into the research domain. Consequently, it can lead to the more effective development of prediction models of thermal properties.

In order to evaluate the development of the research regarding property predictions using machine learning, a bibliometric study in the Web of Science database was performed. The following query was used: (“concrete”) AND (“properties” OR “thermal conductivity”) AND (“machine learning” OR “deep learning” OR “artificial neural network” OR “ANN”). The search criteria used in this bibliometric study summarized 1673 articles and reviewed articles published between 2014 and 2023. Then, the overall result was imported into VOSviewer to analyze the keywords in each paper’s title or abstract. This generated the overlay cluster representing the development of the research over the years (Figure 1).

Figure 1 depicts the relationship between machine learning models and the properties of concrete. Although the documents’ timeline is longer, the figure shows a shorter and more recent timeline due to the many published papers. It is possible to observe several machine learning techniques being used to predict the properties of concrete, in addition to other mathematical models such as genetic algorithms, particle swarm, and adaptive neuro-fuzzy inference systems. The models include random forest, support vector machine, extreme gradient boosting, and neural networks. Furthermore, different properties such as slump, compressive strength, porosity, and thermal conductivity are observed, and the different types of concrete studied include geopolymer, ultra-high-performance concrete, self-compacting concrete, and recycled aggregate concrete. Hence, machine learning models are a state-of-the-art research line with great expectations for development in this area. The efficacy of neural networks, which remain widely employed, is particularly notable in the present context.

Therefore, after the literature and the bibliographic review, we noticed a gap in prediction models regarding thermal properties using machine learning models. This study aims to fill this gap and develop a method to predict the thermal conductivity of concrete. Additionally, we intend to build a model for data augmentation, which has been used in many fields.

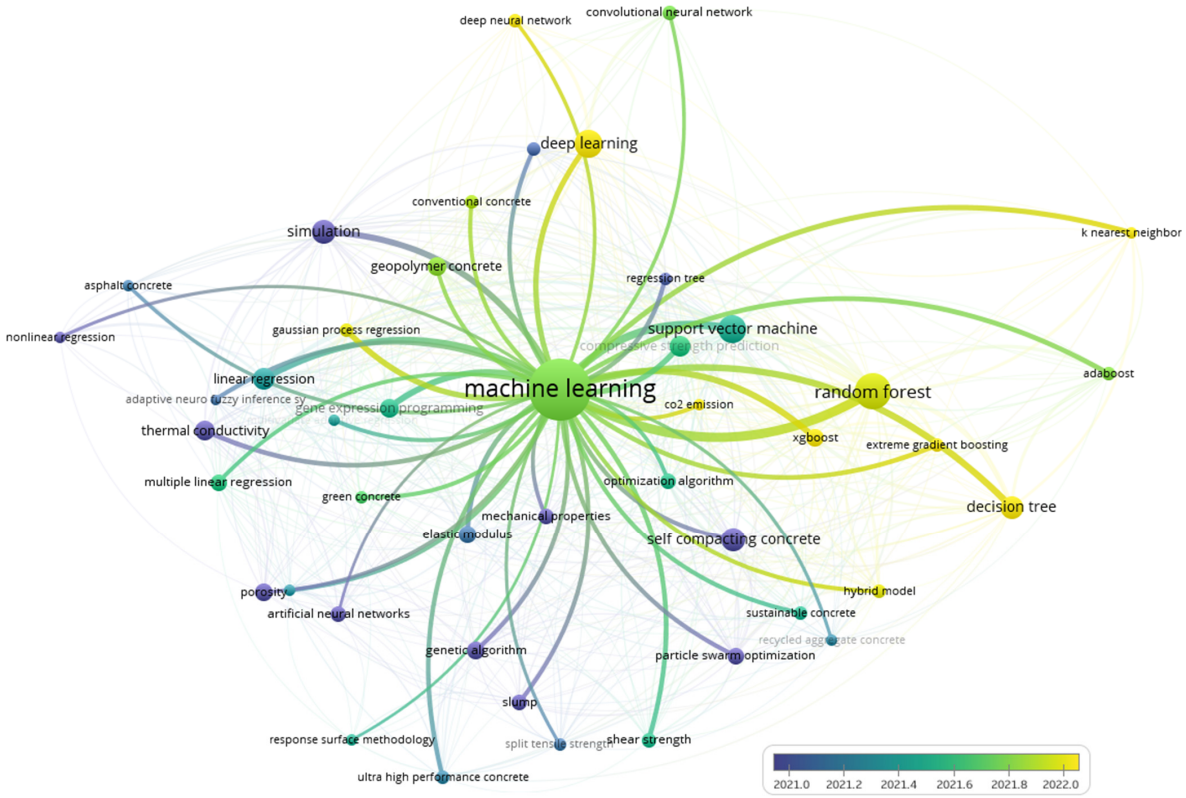

Figure 1. Cluster based on keywords (network visualization).

3. Methodology

The proposed methodology encompasses two primary components: the development of an MLP for material property prediction based on its features and the utilization of a GAN for data augmentation to enhance the dataset and improve the accuracy of the first model. This section outlines the proposed methodology applied to this work to achieve these objectives, broken down into three steps: data collection, model development, and the model's application in a case study (Figure 2).

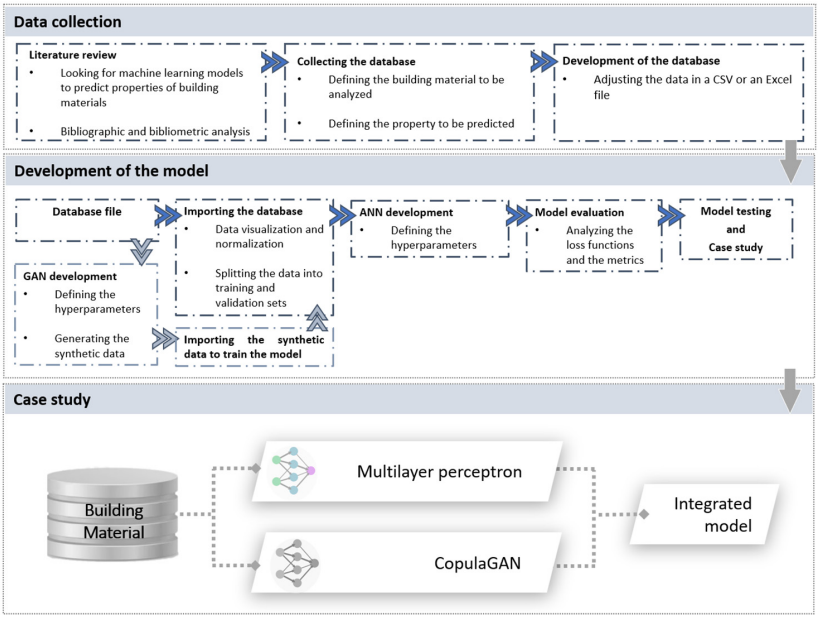

Figure 2. Methodology framework.

3.1. Data Collection

The first step corresponds to a literature review and gathering the database from diverse sources, including industry databases, research publications, and laboratory experiments. Collecting the database is the primordial step in building the predictive model, as the ANN will learn from these data. If it presents an inadequate representation of the problem, the model cannot predict the property effectively, thus reducing the model's reliability. Furthermore, for the model to be representative, there must be a sufficiently large amount of data to ensure diversity. In this step, it is necessary to recognize which relevant input features potentially impact the model's output response. After this process, all the information must be inserted into a CSV or Excel file.

3.2. Development of the Model

The second step is related to the general process of building the prediction model, i.e., data normalization, the selection of an appropriate neural network architecture for the prediction task, defining the learning rate of the neural network, the number of hidden layers and neurons in each layer, and the metrics to find the best model for the dataset.

3.2.1. Importing the Database

Normalizing the dataset is vital in any deep learning model. Since the database may present the parameters in a different and wide range of values, it is necessary to normalize them by putting all features on a standard scale to avoid the data values affecting the weights and biases during the training of the model. Generally, the normalization process transforms the input and output parameters, putting them on a standardized scale, i.e., transforming them to have a mean of zero and a standard deviation of one. This step guarantees that each parameter will contribute equally during the learning process and prevents any parameter from dominating this process due to its more extensive scale. Another advantage is that it enhances the generalization capabilities of the models, improving the prediction of new data. The normalization known as z-score is commonly used to bring the numerical features to the same scale. The mathematical equation of this process is presented in Equation (1).

$$z = (x - \mu)/\sigma, \tag{1}$$

where z is the normalized value, x is the number we would like to normalize, μ is the mean, and σ is the standard deviation of this parameter. Therefore, in order to achieve the normalized values for each numeric column, the mean and the standard deviation are calculated. Each value in the numeric column is subtracted by the column's mean and then divided by the column's standard deviation.

3.2.2. Performance Metrics

Assessing the model's performance is critical to data analysis and predictive modeling. Since each metric provides a unique perspective on different aspects of the model, it is crucial to evaluate more than one metric to achieve a comprehensive and well-rounded assessment of the model's performance, which will give a complete picture of the problem and allow us to gain insights into the strengths and weaknesses of the model.

To quantify the predictive capabilities of the proposed model and enable meaningful comparisons among the different architectures and previous models published in the literature, it is advisable to use more than one performance metric. Researchers commonly employ complementary performance metrics, such as the coefficient of determination (R^2) and root mean squared error (RMSE). The former measures the proportion of the variance in the output that is predictable from the input variables. Its value varies from 0 to 1, and the closer the value is to 1, the better the model's capability to explain the variability of the data. However, the latter measures the average error between the predicted and actual output values. Due to its squared term, it is more sensitive to outliers and more

significant errors. The lower this metric is, the more accurate the predictions are. These metrics are valuable indicators of how well the models capture the data's variance and their predictions' accuracy. The mathematical formulae for R^2 and RMSE are provided in Equations (2) and (3).

$$R^2 = \frac{\sum_{k=1}^{n}(y - y')^2}{\sum_{k=1}^{n}(y - y_m)^2}, \quad (2)$$

$$RMSE = \sqrt{\frac{\sum_{i=1}^{n}(y - y')^2}{n}}, \quad (3)$$

where n is the number of data points, y is the experimental data found in the literature, y' is the predicted data, and y_m is the mean of the experimental data.

3.2.3. Multilayer Perceptron Model

A Multilayer Perceptron (MLP) is an artificial neural network that can be applied to solve many problems, including classification, regression, and pattern recognition. A typical MLP model comprises three blocks of interconnected neurons: the input layer in which each neuron represents a data feature; the hidden layers that could have one or more layers depending on the complexity of the problem; and the output layer, representing the response output (Figure 3). Each neuron in the network is bonded to other neurons through connection weights. Each neuron in a neural network receives an input (X_i) that is multiplied by a weight (W_i) and these are summed with each other and added to the bias value (b). Then, the result is transferred to the activation function, which adjusts the final output (Figure 4). Each layer of neurons gathers input from the previous layers, and the outputs of neurons within one layer become the inputs to neurons in the following layer. Finally, the last layer produces the predictions of the model.

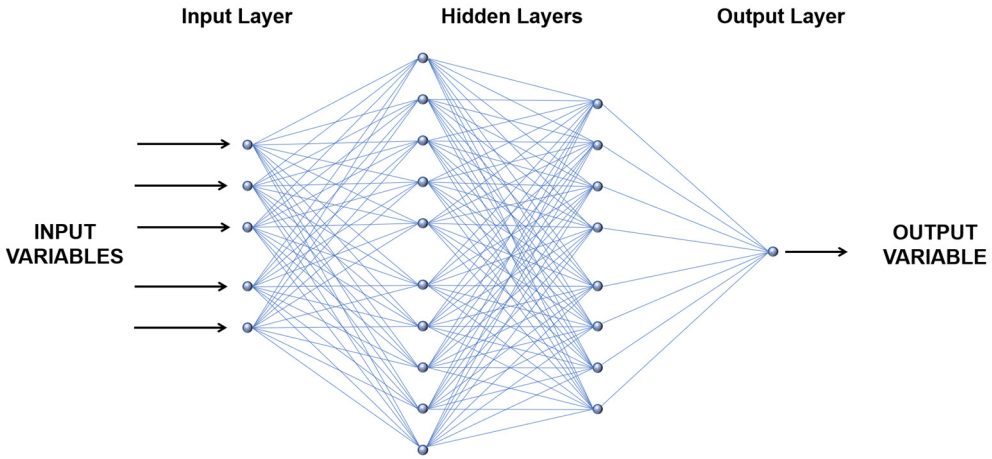

Figure 3. Example of the MLP model.

3.2.4. Generative Adversarial Network Model

A Generative Adversarial Network (GAN) model consists of two distinct neural networks, the generator and the discriminator, which are trained simultaneously. The GAN captures the distribution pattern of a given dataset and generates data that resemble this dataset. First, the generator initiates the process, which takes a random noise as an input, creating samples similar to the original dataset. The discriminator then tries to distinguish the data and detect whether a sample is from the original dataset or the generator model distribution. During the training, the generator loss and the discriminator loss are evaluated, allowing the generator to get better and better at producing new artificial data and the discriminator to find out if they are real or synthetic (Figure 5). This methodology framework used the Copula GAN synthesizer, a CTGAN variation. It uses the cumula-

tive distribution function-based transformation that Gaussian copulas apply, making the learning process easier.

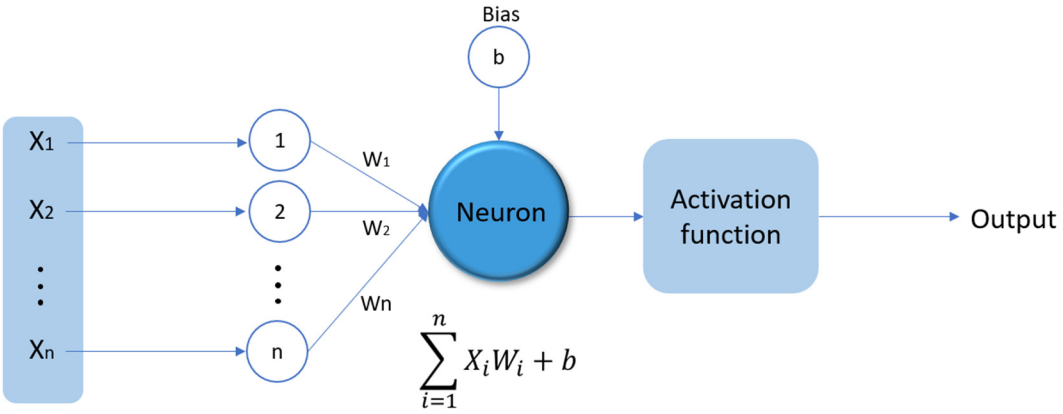

Figure 4. Graphical representation of a neuron.

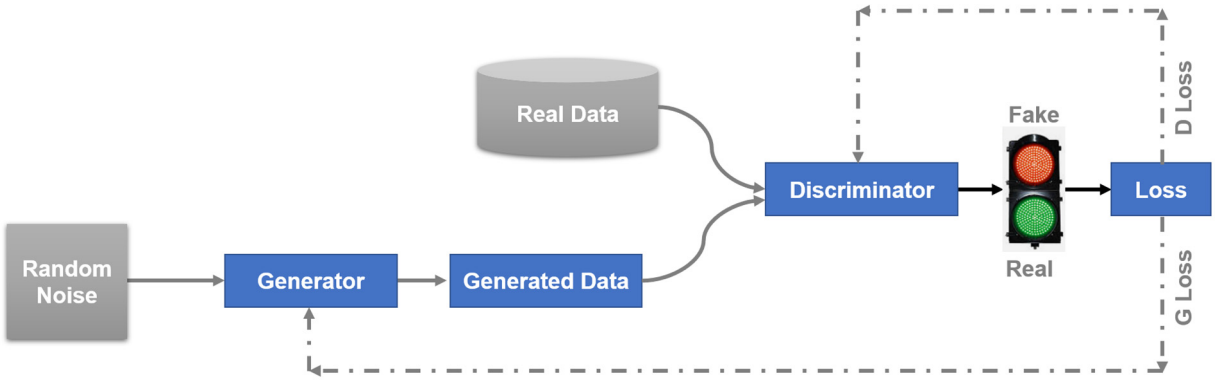

Figure 5. Flowchart of a Generative Adversarial Network (GAN).

3.3. Case Study

The proposed model is applied to conduct a broad case study on concrete mixtures. As previously highlighted in the introduction, precise thermal conductivity predictions for building materials can significantly enhance building thermal performance. Given that the thermal conductivity of concrete can be influenced by the type and quantity of each constituent, this study seeks to predict this critical property based on the mass composition of these constituents.

A comprehensive literature review is conducted to create a database of 200 points compiled from various relevant studies published in the literature. Each selected paper presents a different type of concrete, such as recycled aggregate concrete, lightweight concrete, fiber-reinforced foamed concrete, moderate-strength concrete, and concrete with vermiculite. This variation allows the development of a generalist model. The dataset compiled in this context consists of concrete from 12 sources (Table 2) with modern constituent materials: ceramic, slag, silica fume, fly ash, steel fiber, propylene fiber, recycled aggregate, lightweight aggregate, waste aggregate, and foam. The model's inputs are defined according to the available data and the influence of each feature on the thermal conductivity.

Here, a total of 18 input parameters that affect the output, thermal conductivity, are considered. The selected input parameters for this case study are density (D), water-to-cement ratio (W/C), water content (W), cement content (C), ceramic powder content (Ce), fine aggregate content (FAg), coarse aggregate content (CAg), natural aggregate content (NAg), recycled aggregate content (RAg), light aggregate content (LAg), waste aggregate content (WAg), fly ash content (FA), silica fume content (SF), slag content (S), fiber content (F), other admixture content (Ad), superplasticizer content (Sp), and foam volume content

(FV). The values of TC lie in the range of 0.37–2.70 W/m.K with a standard deviation of 0.5 W/m.K. The dataset used in this study comprises input parameters collected from various independent research groups, each of which conducted studies with different objectives and, consequently, different sets of input variables. As a result, certain parameters that might appear to be missing in Table 2 are not absent; rather, they were simply not included in specific studies due to the varying focuses of each research effort. Therefore, the absence of certain data points in specific groups is by design and does not represent missing values in the conventional sense. Each group of data was used in a complete form relevant to its particular context, ensuring that the model was trained and validated with the available and intended inputs, without the negative impact of non-existent data.

Table 2. The summary of the dataset used in the model.

		Zhu et al. [36]	**Kim et al. [37]**	**Lee et al. [32]**	**Vejmelková et al. [38]**	**Demirboga [39]**	**Sargam et al. [40]**
N° of data		15	14	82	5	9	21
D	[kg/m^3]	1617–2195	1540–2297	1144–3075	2017–2199	2290–2355	1626–2380
W/C	-	0.40–0.50	0.25–0.57	0.22–0.62	0.32–0.80	0.35	0.35–0.55
W	[kg/m^3]	130–150	140–558	133–524	124	167.5	120–190
C	[kg/m^3]	260–375	0–1792	242–1762	154–385	245–324	90–110
Ce	[kg/m^3]	-	-	-	0–231	-	-
FAg	[kg/m^3]	0–658	0–702	0–1167	775	740	280–365
CAg	[kg/m^3]	0–605	0–1103	0–1850	175	458	-
NAg	[kg/m^3]	0–987	-	-	770	577	0–440
RAg	[kg/m^3]	0–1710	-	-	-	-	0–460
LAg	[kg/m^3]	-	-	-	-	-	0–320
WAg	[kg/m^3]	0–1645	-	-	-	-	-
FA	[kg/m^3]	-	0–973	0–104	392	26.25–105	0–30
SF	[kg/m^3]	-	-	0–89	-	26.25–52.5	-
S	[kg/m^3]	-	0–1282	-	-	26.25–105	-
F	[kg/m^3]	-	-	-	-	-	0–20
Ad	[kg/m^3]	-	0–8.81	-	-	-	-
Sp	[kg/m^3]	-	-	-	3.4–4	1.8	-
FV	[kg/m^3]	-	-	-	-	-	-
TC	[W/m.K]	0.74–1.40	0.66–1.69	0.30–2.50	1.21–1.55	0.95–1.17	0.70–1.20
		Sargam et al. [41]	Sargam et al. [42]	Cavalline et al. [43]	Kurpinska et al. [44]	Gencel et al. [31]	Bayraktar et al. [45]
N° of data		4	1	17	4	4	20
D	[kg/m^3]	2281–2367	2389	1434–2219	1234–2244	1194–1370	1418–1988
W/C	-	0.45	0.43	0.29–0.54	0.40	0.63–1.37	0.75–1.88
W	[kg/m^3]	157	151	155–218	220–310	471–580	338
C	[kg/m^3]	349	281	268–454	500–700	422–750	180–450
Ce	[kg/m^3]	-	-	-	-	-	-
FAg	[kg/m^3]	772–821	890	0–1559	0–1300	-	0–1091
CAg	[kg/m^3]	-	-	-	-	149–192	-
NAg	[kg/m^3]	0–1171	900	0–1068	-	-	-
RAg	[kg/m^3]	0–1036	-	-	-	-	-
LAg	[kg/m^3]	-	-	0–1101	-	-	-
WAg	[kg/m^3]	-	-	-	0–490	-	0–1091
FA	[kg/m^3]	-	71	0–102	-	-	-
SF	[kg/m^3]	-	-	-	-	-	-
S	[kg/m^3]	-	-	-	-	-	0–270
F	[kg/m^3]	-	-	-	-	-	0–9
Ad	[kg/m^3]	-	-	-	-	-	-
Sp	[kg/m^3]	-	-	-	3–4.9	-	-
FV	[kg/m^3]	-	-	-	-	-	50–100
TC	[W/m.K]	0.89–1.14	2.70	0.69–1.78	0.37–1.19	0.33–0.52	0.50–0.75

In order to train the model, the compiled dataset is randomly divided into training (80%) and validation sub-dataset (20%). Then, the reliability and reproducibility of the ANN model are evaluated on a new testing dataset. The predictive performance of the final model is thoroughly assessed using the metrics mentioned above. This assessment allows us to check the model's accuracy and efficiency in capturing the underlying patterns within the database.

4. Results and Discussion

This section presents the model specifications, performance metrics, and outcomes derived from the implementation analysis of deep neural networks. The results are organized into three subsections: firstly, the implementation of the Multilayer Perceptron (MLP) model in Python; secondly, an assessment of the feasibility of generating synthetic data using CopulaGAN; and lastly, the training and evaluation of the MLP model with two distinct datasets.

4.1. Development of the Multilayer Perceptron Model

The primary objective of this work is to develop an MLP model for predicting the thermal conductivity of concrete based on its mass composition and density. The hyperparameters of the MLP model are initially predefined and subsequently fine-tuned to enhance the prediction accuracy. Table 3 provides an overview of the model's key features, encompassing the hyperparameters, evaluation metrics, activation functions, optimization methods, and loss functions.

Table 3. Main features of the MLP model.

1. Hyperparameters	Hidden layers = [1, 2, 3, 4] Batch size = 64 Learning rate = 0.001 Epochs = 100
2. Metrics	RMSE R^2
3. Activation function	ReLU
4. Optimization function	Stochastic Gradient Descent (SGD)
5. Loss function	MSE

To establish the optimal architecture of the MLP model, the number of hidden layers and neurons is systematically varied, and a combination of the metrics RMSE and R^2 is employed to measure the model's overall performance. A diligent trial-and-error approach is undertaken to determine the most effective configuration for the number of hidden layers and neurons in each layer. Table 4 displays the loss functions and performance metrics of the multiple neural networks assessed in this study. Notably, the most proficient model features a two-hidden-layer structure with 200 and 100 neurons, yielding an RMSE of 0.111 W/m.K and an R^2 of 0.984 for the training dataset. As for the validation dataset, the model demonstrates metrics values of 0.183 and 0.960, respectively.

Table 4. Performance indices and metrics of the MLP model.

Layers	ANN Architecture	Train Loss	Valid Loss	RMSE	R^2
4	200–100	0.083	0.012	0.111	0.984
5	200–100–50	0.107	0.024	0.155	0.968
5	200–100–40	0.099	0.037	0.192	0.950
5	200–100–30	0.087	0.028	0.167	0.960
5	200–100–20	0.012	0.037	0.191	0.949
6	200–100–50–25	0.102	0.064	0.253	0.918

Regarding the best-performing model, an analysis of the loss functions and the performance metrics versus the number of epochs is conducted (Figure 6). As the number of epochs progresses, a significant pattern appears in the training and validation processes. Both training and validation losses exhibit an exponential decrease as iterations continue. In parallel, the performance metrics on the validation dataset align with the behavior of the loss function. While RMSE steadily declines, R^2 shows a corresponding increase, achieving its minimum and maximum value at approximately 100 epochs. This observed trend reflects the model's capacity to optimize its predictive accuracy as it refines its learning over successive epochs.

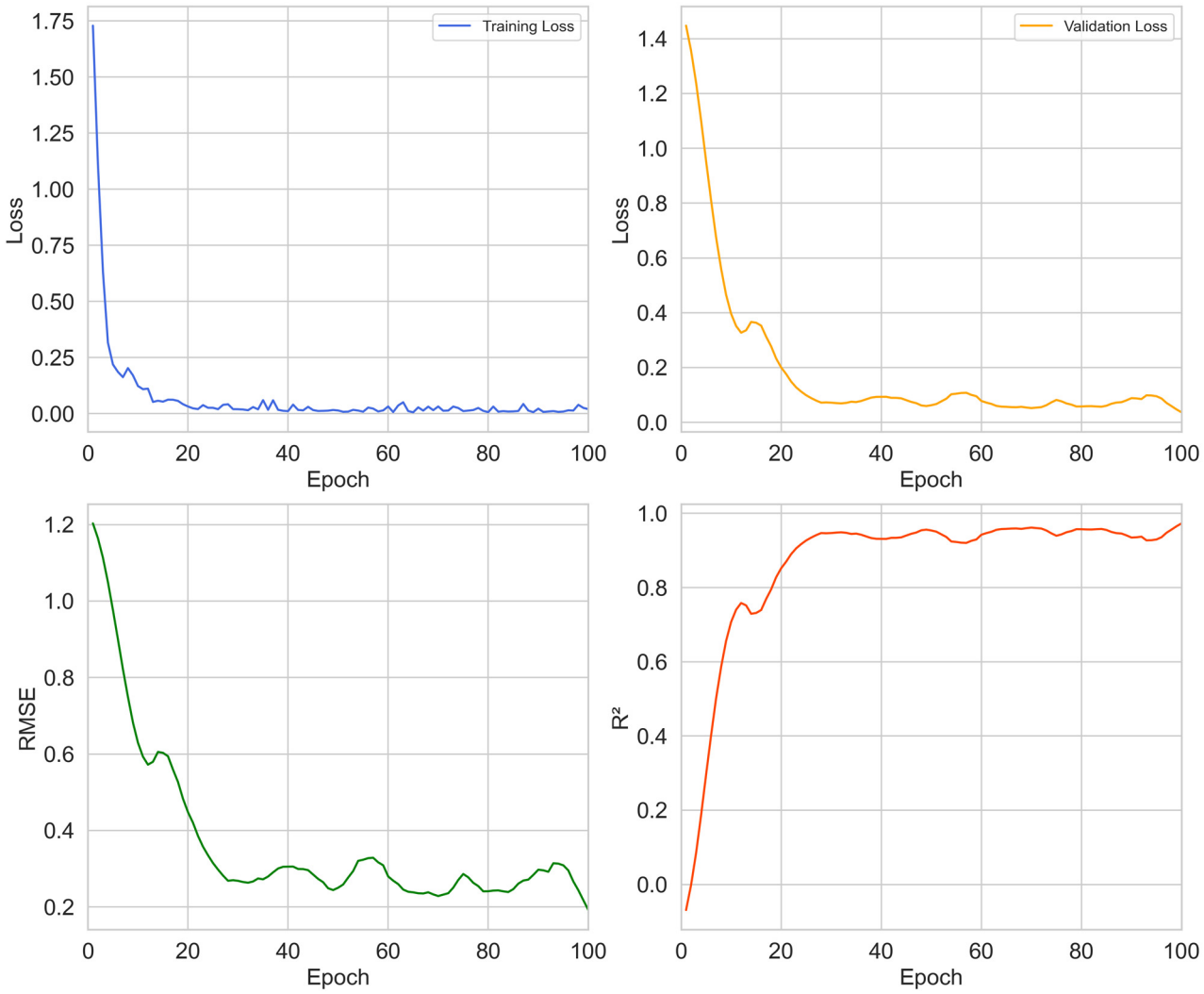

Figure 6. Loss function and performance measures during the training and validation.

Comparing the findings of the MLP model to previous studies, they demonstrate a remarkable level of accuracy for the training and validation. A study by Fidan et al. [28], using a dataset with 132 entries, developed an ANN based on the mechanical properties and the density of concrete, which had an overall R^2 performance of 0.996. However, the ANN architecture used only one hidden layer with 5 to 25 neurons. Sargam et al. [6] took a step further by implementing a neural network with a larger dataset, with an RMSE of 0.117 and R^2 of 0.964 for the training set and an RMSE of 0.215 and R^2 of 0.894 for the validation set. Nonetheless, large residuals were obtained. Another high-performance ANN model was developed by Gencel et al. [31] where they investigated the influence of concrete composition and temperature on thermal conductivity. Despite the results of an R^2 of 0.998 and RMSE of 0.005 during neural network training, only 12 inputs were used.

Although these works showed substantial success in predicting thermal conductivity, our model upholds higher accuracy and introduces a broader array of concrete constituents into the modeling process.

4.2. Development of the Generative Adversarial Network Model

The second part of the study considers the implementation of CopulaGAN for data augmentation. As can be observed in Table 4, increasing the number of layers does not improve the model's learning capacity or performance. If we increase the hidden layers of the model with a small dataset, the model can overfit. For this reason, the loss functions exhibit higher values. In order to solve this issue, we intend to develop a GAN model to increase the dataset, creating new synthetic data based on the real data used to develop the MLP model. This will avoid the overfitting process and make the model more robust with extensive dataset training.

After generating the synthetic data, two aspects of the original data were evaluated: the column shapes and pair trends. Each aspect contributed differently to the overall score, which reached 78.14%, indicating that the synthetic data has acceptable quality. In Figure 7, we present the distribution of the augmented dataset. It illustrates the distribution of normalized thermal conductivity values for both real and synthetic datasets. The real data, shown in dark blue, have a sharper peak, while the synthetic data, depicted in light blue, exhibit a similar peak but with a slightly different spread. The overlap between the two distributions indicates that the synthetic data generated by CopulaGAN are largely representative of the real data, despite some discrepancies.

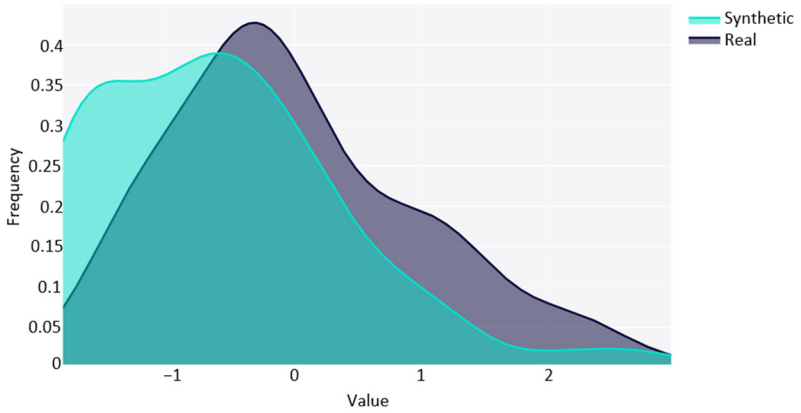

Figure 7. Distribution of the synthetic generated by GAN and the real data.

After the synthetic data generation, we aim to incorporate it into the MLP model for joint training with real and artificial datasets. To assess the model's response to this diverse training approach, two distinct sets of synthetic data were created, one comprising 200 data points and the other consisting of 1000 data points. The seamless integration of these two neural network models and the subsequent validation of the model using a new test set are elaborated upon in the forthcoming section.

Statistical Evaluation of the Generative Adversarial Network Model

To assess the quality of the synthetic data, two metrics were utilized: the Correlation Matrix Comparison and the Kolmogorov–Smirnov Test (KS Test). The Correlation Matrix Comparison examines whether the relationships between variables in the synthetic dataset are consistent with those in the real dataset. The KS Test, on the other hand, compares the distributions of the two datasets to determine if they are drawn from the same underlying distribution.

According to Table 5, several key observations can be made. Variables with high KS scores, such as density (0.913), cement (0.883), superplasticizer (0.923), and thermal conductivity (tc) (0.883), indicate that the synthetic data closely resemble the real data for

these variables. Moderate scores, including water/cement ratio (0.781), water (0.806), and fine aggregate (0.867), show good correspondence, though the match is slightly less precise. However, lower scores for variables like ceramic powder (0.541), natural aggregate (0.515), fly ash (0.480), and light aggregate (0.388) suggest that the synthetic data do not replicate these distributions as effectively, highlighting potential areas for improvement in the data generation model.

Table 5. KS Test evaluation.

Column	Score
Density	0.9133
w/c ratio	0.7806
Water	0.8061
Cement	0.8827
Ceramic powder	0.5408
Fine agg.	0.8673
Coarse agg.	0.6684
Natural agg.	0.5153
Recycled agg.	0.8622
Light agg.	0.3878
Waste agg.	0.6480
Fly ash	0.4796
Silica fume	0.6480
Slag	0.5357
Fiber	0.5918
Admix.	0.5255
Superplast.	0.9235
Foam volume	0.5000
tc	0.8827

In the Correlation Matrix Comparison, the analysis focuses on the similarity between the correlations in the real and synthetic datasets. A score closer to 1 indicates a stronger resemblance. The majority of variable pairs have high correlation similarity scores, typically above 0.95, signifying that the synthetic data effectively mirror the correlation structure of the real data. For example, the correlation between density and cement shows a score of 0.979, with real and synthetic correlations being -0.118 and -0.078, respectively, suggesting that the synthetic data closely capture this relationship.

However, while the correlation similarity scores are generally high, there are differences in the exact correlation values between some pairs. For instance, the correlation between density and water/cement ratio is -0.391 in the real data but only -0.201 in the synthetic data, despite a correlation similarity score of 0.905. This indicates that although the general trend is captured, the synthetic data do not fully replicate the strength of the relationship.

Overall, the synthetic data generation process effectively replicates the correlation structure found in the real data, though there are some deviations in the exact correlation values. These discrepancies suggest that while the synthetic data are generally reliable, some relationships might not be fully captured, particularly where the real data show weaker or more nuanced correlations. Further refinement of the synthetic data generation process could help better match these subtle relationships.

4.3. Integration of Both Models to Predict Thermal Conductivity

The third phase of this study is dedicated to examining the impact of synthetic data on the training of a neural network model. This evaluation is conducted to ascertain whether a model trained with augmented data can produce results comparable to the performance achieved through training with real data and possibly enhance it. In order to assess this impact, this study investigates three distinct scenarios: (a) training the MLP model exclusively with the real dataset containing 200 entries, (b) training the model with

the synthetic data consisting of 200 entries first and subsequently incorporating the real dataset, and (c) training the model with 1000 data points of the synthetic data and then integrating the real dataset.

The same hyperparameters utilized in developing the final model are maintained in this integration process. The key distinction lies in the dataset used for the training and validation phases. Our approach initially involves training the model first with synthetic data. Subsequently, the same model architecture uses the real dataset to enhance the model's performance. The results for the previous MLP model (a) and scenarios (b) and (c) are summarized in Table 6, indicating the outcomes of the final model.

Table 6. Performance metrics of the MLP model trained with both datasets.

Scenario	Dataset	Overall	
		RMSE	**R^2**
(a)	Training	0.0443	0.9923
	Validation	0.3233	0.9228
	Test	0.0604	0.9846
(b)	Training	0.0221	0.9980
	Validation	0.1329	0.9870
	Test	0.0439	0.9919
(c)	Training	0.0219	0.9981
	Validation	0.0735	0.9960
	Test	0.0244	0.9975

The predictive capabilities of the developed model are thoroughly examined using a new dataset comprising 30 data points to assess its generalization performance. Despite the limited size of the dataset in scenario (a), the training and validation phases yield commendable results, with an RMSE of 0.0604 and an R^2 of 0.9846. In scenarios (b) and (c), where synthetic data play a vital role, both demonstrate exemplary performance during training, achieving R^2 values of 0.9995 and 0.9962. This improvement in the results also extends to the validation dataset, with R^2 values of 0.9938 and 0.9754. Post-incorporation of real data into the training process, the metrics exhibit comparable values during training and improvements in validation, 0.9870 and 0.9960 for scenarios (b) and (c), respectively. Upon rigorous evaluation of the independent test set, scenario (c) emerges as the most robust and indicates the most favorable combination of performance metrics.

The predictive performance of the developed MLP model for the three scenarios is evaluated on an independent test dataset that can be graphically seen in Figures 8 and 9. Comparing the actual and predicted thermal conductivity results for each scenario, a distinct pattern emerges, underscoring the model's significant performance enhancement when integrated with synthetic data. In Figure 8a, we present the predictions for the first case, wherein a considerable portion of the points align with the ideal x = y line. However, some deviations are noticeable, with errors exceeding 0.12. Figure 8b,c illustrate scenarios where the model is trained using synthetic data. In both instances, incorporating synthetic data leads to a discernible improvement in prediction accuracy and a notable error reduction. Scenario (c) stands out, boasting a larger dataset and delivering the most compelling outcomes. This scenario achieves the optimal combination of performance metrics, represented by a best-fit line with an impressive R^2 value of 0.9975 and a minimal RMSE of 0.0244.

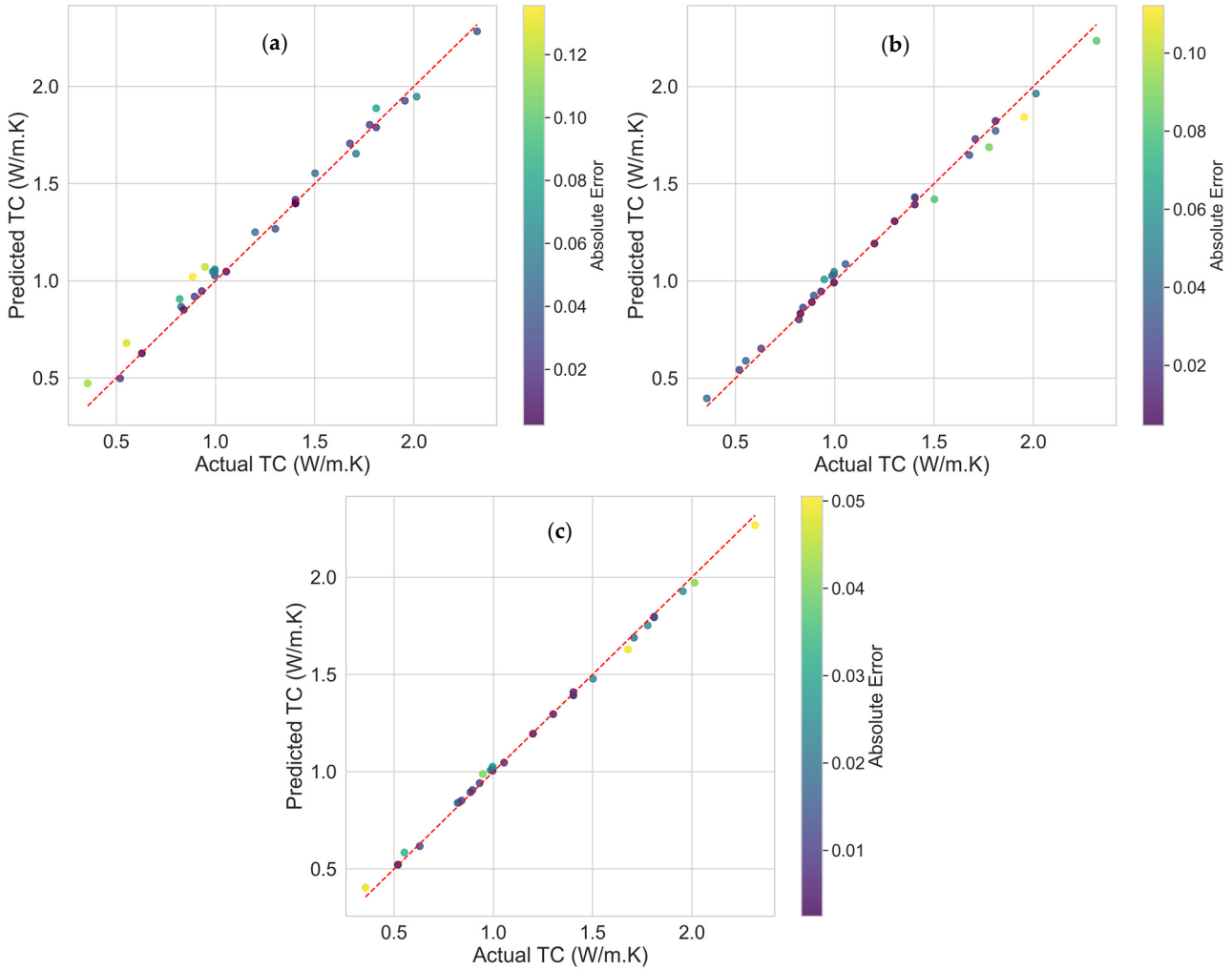

Figure 8. Performance and predictions of the thermal conductivity of the test dataset for the three scenarios: (**a**) training the model with real data only, (**b**) training the model with 200 synthetic data points and real data, and (**c**) training the model with 1000 synthetic data points + real data.

Figure 9 shows the relationship between the actual values derived from the test dataset from published papers and the corresponding predictions generated by the Multilayer Perceptron (MLP) model. This visual representation allows us to assess the model's accuracy in forecasting thermal conductivity, providing valuable insights into its performance.

In Figure 9a, we depict the model utilizing solely the real dataset, while Figure 9b,c display the model trained with both the 200-point and 1000-point datasets, respectively. Although Figure 9a reveals a close alignment between predicted and real points, some discrepancies across various data points with errors as high as 0.13 and 0.14 W/m.K observed. Moving to Figure 9b, a significant reduction in these discrepancies becomes evident, especially within the low thermal conductivity values spanning from 0.5 to 1.0 W/m.K in range. This evidence signifies a marked improvement in prediction accuracy, resulting in a substantial decrease in both the number of points with errors and the magnitude of these errors, reducing the maximum error to 0.11 W/m.K. Figure 9c unveils an even more prominent enhancement in accuracy, with predictions exhibiting a higher level of precision and a further reduction in errors. In this case, the most significant error recorded is 0.05 W/m.K.

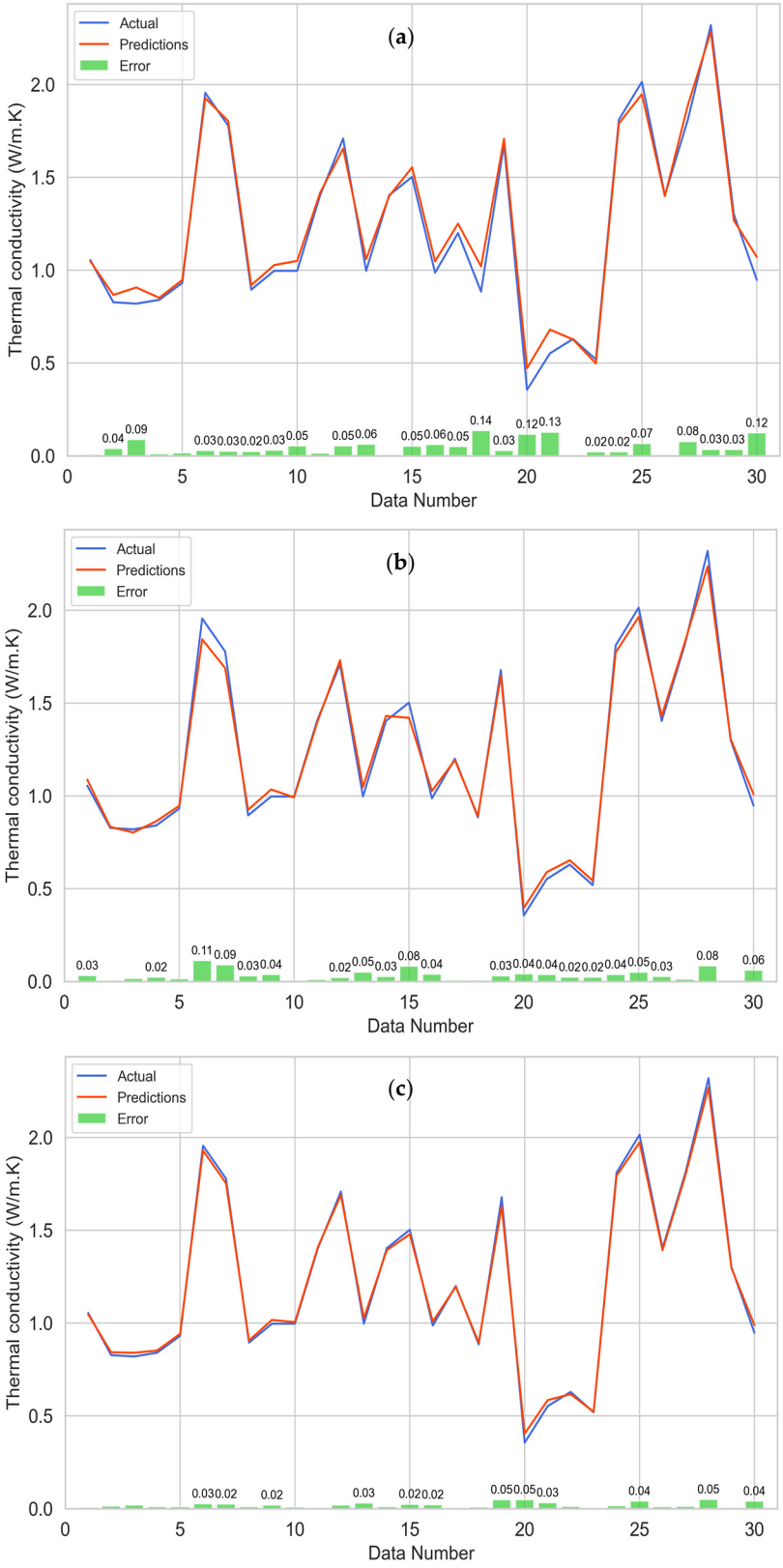

Figure 9. Comparison of actual thermal conductivity with model predictions across different training scenarios: (**a**) training the model with real data only, (**b**) training the model with 200 synthetic data points and real data, and (**c**) training the model with 1000 synthetic data points + real data.

In summary, an impressive alignment between the actual and predicted values is achieved across all three cases. The first case exhibits a comparatively lower performance than the other two, potentially attributed to the limited size of the dataset. The presence of a smaller database may result in a more significant deviation between actual and predicted values, particularly within the thermal conductivity range of 0.5–1.0 W/m.K. This scarcity of data becomes apparent when synthetic data are introduced for training, ultimately enhancing the model's accuracy in predicting the thermal conductivity property.

The methodology employed in this study endeavors to show the efficacy of neural networks in predicting the thermal properties of concrete based on the mass composition of its constituents. Furthermore, it seeks to investigate the utilization of synthetic data generation for training neural networks, addressing the challenge of data scarcity, a significant impediment to the accuracy of models employing machine or deep learning techniques. While the existing literature demonstrates notable success in utilizing neural networks for thermal conductivity prediction, our model achieves higher accuracy and incorporates a more extensive array of concrete constituents into the modeling process. This diversity enhances the model's versatility, expanding its applicability to a broader range of materials.

5. Conclusions

This study proposed a comprehensive methodology using deep neural networks. In the initial phase, various architectures of a Multilayer Perceptron were explored, and the most effective one was selected for an in-depth case study. Subsequently, we introduced a Generative Adversarial Network to create synthetic datasets, facilitating the training of the Multilayer Perceptron with both real and synthetic data. The application of this methodology was specifically demonstrated in the context of concrete mixtures. The dataset was meticulously gathered from published papers.

For a comprehensive evaluation of the case study, we compared and assessed three distinct scenarios: (a) training the MLP exclusively with the real database, (b) training the MLP with 200 synthetic data points followed by real data, and (c) training the MLP with 1000 synthetic data points followed by real data. The outcomes across all three scenarios demonstrated satisfactory and highly accurate predictions of concrete thermal conductivity. Notably, including synthetic data in the training process led to a remarkable enhancement in accuracy and a significant reduction in errors within the test dataset, which underscores the effectiveness of the CopulaGAN synthesizer in generating synthetic data and the efficiency of MLP training with a combined dataset. The evaluation of these scenarios utilized the performance metrics RMSE and R^2, yielding the following values for each scenario: scenario (a)—0.0581 and 0.9858; scenario (b)—0.0394 and 0.9935; and scenario (c)—0.0314 and 0.9959, respectively.

This study aimed to develop a methodology for predicting the thermal properties of concrete using artificial neural networks. Our specific focus was to demonstrate the feasibility of forecasting concrete's thermal conductivity based on its constituents' mass composition. Additionally, we sought to show the benefits of integrating a Generative Adversarial Network for data augmentation. The implications of this study can offer insights that can be applied to the development and enhancement of prediction models using deep learning for other materials. One notable impact lies in advancing the field of energy efficiency in buildings, providing decision-makers and manufacturers with advanced knowledge of a building material's thermal properties. While this work has made valuable contributions, it is essential to acknowledge certain limitations. Notably, this study could be enhanced by including other influential input variables, such as temperature, aggregate types, and mineralogy, and by expanding the real dataset to improve predictions across a broader range of thermal conductivity values. Besides this, although the results are promising, we agree that additional validation using independent datasets would further strengthen the reliability of our findings. Future work will focus on validating the model using experimental setups to further ensure its generalizability and accuracy. Moreover, future research studies could explore the application of this methodology to

other composite materials and consider the inclusion of additional information, such as mechanical properties. An additional option is to explore specific heat as an output variable, a fundamental property in transient conditions, complementing the importance of thermal conductivity in stationary scenarios. This way, we can understand how different materials behave and make the predictions even more accurate. This work underscores the importance of training models with sufficiently diverse datasets to ensure accuracy, and it highlights the potential of synthetic data to augment training when faced with a scarcity of real data.

Author Contributions: The authors confirm contributions to the paper as follows: study conceptualization and methodology: C.M., A.C. and D.B.; data collection, software validation, analysis, and interpretation of results: A.C.R. and Y.E.; original draft preparation: A.C.R.; writing, reviewing, and editing: A.C.R., A.C. and D.B.; supervision: D.B. and A.H. All authors have read and agreed to the published version of the manuscript.

Funding: The authors would like to acknowledge financial support from the Coordenação de Aperfeiçoamento de Pessoal de Nível Superior (CAPES), Finance Code 001, Conselho Nacional de Desenvolvimento Científico e Tecnológico (CNPq), Fundação de Amparo à Pesquisa do Estado do Rio de Janeiro (Faperj) 2019-E-26/202.568/2019 (245653), and "Ministerio de Ciencia, Innovación y Universidades" of Spain [PID2021-127713OA-I00, PID2021-123511OB-C32, PID2021-123511OB-C33, PID2021-124139NB-C22-MCIN/AEI/10.13039/501100011033/FEDER, EU, TED2021-129851B-I00-/AEI/10.13039/501100011033/Unión Europea NextGenerationEU/PRTR and RED2022-134219-T].

Institutional Review Board Statement: Not applicable.

Informed Consent Statement: Not applicable.

Data Availability Statement: The original contributions presented in the study are included in the article, further inquiries can be directed to the corresponding author.

Conflicts of Interest: The authors declare no conflicts of interest.

Nomenclature

Symbols	
Coefficient of determination	R^2
Density—D	ρ [kg/m^3]
Experimental data found in the literature	y
Mean of the experimental data	y_m
Mean of the normalized value	
Normalized value	z
Number of data points	n
Number to be normalized	x
Predicted data	y'
Root mean squared error	$RMSE$
Standard deviation	σ
Thermal conductivity—TC	k [W/m.K]

References

1. Park, S.H.; Chung, J.; Yeo, M.S.; Kim, K.W. Evaluation of the thermal performance of a Thermally Activated Building System (TABS) according to the thermal load in a residential building. *Energy Build.* **2014**, *73*, 69–82. [CrossRef]
2. Zhang, D.; Li, Z.; Zhou, J.; Wu, K. Development of thermal energy storage concrete. *Cem. Concr. Res.* **2004**, *34*, 927–934. [CrossRef]
3. Wu, M.; Li, M.; Xu, C.; He, Y.; Tao, W. The impact of concrete structure on the thermal performance of the dual-media thermocline thermal storage tank using concrete as the solid medium. *Appl. Energy* **2014**, *113*, 1363–1371. [CrossRef]
4. DeRousseau, M.A.; Kasprzyk, J.R.; Srubar, W.V. Computational design optimization of concrete mixtures: A review. *Cem. Concr. Res.* **2018**, *109*, 42–53. [CrossRef]
5. Wang, S.; Abdulridha, A.; Bravo, J.; Naito, C.; Quiel, S.; Suleiman, M.; Romero, C.; Neti, S.; Oztekin, A. Thermal energy storage in concrete: Review, testing, and simulation of thermal properties at relevant ranges of elevated temperature. *Cem. Concr. Res.* **2023**, *166*, 107096. [CrossRef]

6. Sargam, Y.; Wang, K.; Cho, I.H. Machine learning based prediction model for thermal conductivity of concrete. *J. Build. Eng.* **2021**, *34*, 101956. [CrossRef]
7. Ullah, H.S.; Khushnood, R.A.; Ahmad, J.; Farooq, F. Predictive modelling of sustainable lightweight foamed concrete using machine learning novel approach. *J. Build. Eng.* **2022**, *56*, 104746. [CrossRef]
8. Behnood, A.; Golafshani, E.M. Machine learning study of the mechanical properties of concretes containing waste foundry sand. *Constr. Build. Mater.* **2020**, *243*, 118152. [CrossRef]
9. Han, T.; Siddique, A.; Khayat, K.; Huang, J.; Kumar, A. An ensemble machine learning approach for prediction and optimization of modulus of elasticity of recycled aggregate concrete. *Constr. Build. Mater.* **2020**, *244*, 118271. [CrossRef]
10. Mehta, V. Machine learning approach for predicting concrete compressive, splitting tensile, and flexural strength with waste foundry sand. *J. Build. Eng.* **2023**, *70*, 106363. [CrossRef]
11. Ji, T.; Lin, T.; Lin, X. A concrete mix proportion design algorithm based on artificial neural networks. *Cem. Concr. Res.* **2006**, *36*, 1399–1408. [CrossRef]
12. Song, H.W.; Kwon, S.J. Evaluation of chloride penetration in high performance concrete using neural network algorithm and micro pore structure. *Cem. Concr. Res.* **2009**, *39*, 814–824. [CrossRef]
13. Huo, Z.; Wang, L.; Huang, Y. Predicting carbonation depth of concrete using a hybrid ensemble model. *J. Build. Eng.* **2023**, *76*, 107320. [CrossRef]
14. Cai, R.; Han, T.; Liao, W.; Huang, J.; Li, D.; Kumar, A.; Ma, H. Prediction of surface chloride concentration of marine concrete using ensemble machine learning. *Cem. Concr. Res.* **2020**, *136*, 106164. [CrossRef]
15. Moein, M.M.; Saradar, A.; Rahmati, K.; Mousavinejad, S.H.G.; Bristow, J.; Aramali, V.; Karakouzian, M. Predictive models for concrete properties using machine learning and deep learning approavhes: A review. *J. Build. Eng.* **2023**, *63*, 105444. [CrossRef]
16. Naderpour, H.; Rafiean, A.H.; Fakharian, P. Compressive strength prediction of environmentally friendly concrete using artificial neural networks. *J. Build. Eng.* **2018**, *16*, 213–219. [CrossRef]
17. Li, X.; Liu, S.; Zhao, L.; Meng, X.; Fang, Y. An integrated building energy performance evaluation method: From parametric modeling to GA-NN based energy consumption prediction modeling. *J. Build. Eng.* **2022**, *45*, 103571. [CrossRef]
18. Al-shawafi, A.; Zhu, H.; Haruna, S.I.; Bo, Z.; Laqsum, S.A.; borito, S.M. Experimental study and machine learning algorithms for evaluating the performance of U-shaped ultra-high performance reinforced fiber concrete under static and impact loads. *J. Build. Eng.* **2023**, *70*, 106389. [CrossRef]
19. Sharifi, Y.; Hosseinpour, M. Compressive strength assessment of concrete containing metakaolin using ANN. *J. Rehabil. Civ. Eng.* **2020**, *8*, 15–27. [CrossRef]
20. Goodfellow, I.J.; Pouget-Abadie, J.; Mirza, M.; Xu, B.; Warde-Farley, D.; Ozair, S.; Courville, A.; Bengio, Y. Generative Adversarial Nets. *Adv. Neural Inf. Process. Syst.* **2014**, *27*, 2672–2680. [CrossRef]
21. Xu, L.; Skoularidou, M.; Cuesta-Infante, A.; Veeramachaneni, K. Modeling Tabular Data using Conditional GAN. *Adv. Neural Inf. Process. Syst.* **2019**, *32*. [CrossRef]
22. Abedi, M.; Hempel, L.; Sadeghi, S.; Kirsten, T. GAN-Based Approaches for Generating Structured Data in the Medical Domain. *Appl. Sci.* **2022**, *12*, 7075. [CrossRef]
23. Yeh, I.-C. Modeling of strength of high-performance concrete using artificial neural networks. *Cem. Concr. Res.* **1998**, *28*, 1797–1808. [CrossRef]
24. Yeh, I.-C. Modeling slump flow of concrete using second-order regressions and artificial neural networks. *Cem. Concr. Compos.* **2007**, *29*, 474–480. [CrossRef]
25. Kandiri, A.; Golafshani, E.M.; Behnood, A. Estimation of the compressive strength of concretes containing ground granulated blast furnace slag using hybridized multi-objective ANN and salp swarm algorithm. *Constr. Build. Mater.* **2020**, *248*, 118676. [CrossRef]
26. Abellán-García, J. Four-layer perceptron approach for strength prediction of UHPC. *Constr. Build. Mater.* **2020**, *256*, 119465. [CrossRef]
27. García, J.A.; Gómez, J.F.; Castellanos, N.T. Properties prediction of environmentally friendly ultra-high-performance concrete using artificial neural networks. *Eur. J. Environ. Civ. Eng.* **2022**, *26*, 2319–2343. [CrossRef]
28. Fidan, S.; Oktay, H.; Polat, S.; Ozturk, S. An Artificial Neural Network Model to Predict the Thermal Properties of Concrete Using Different Neurons and Activation Functions. *Adv. Mater. Sci. Eng.* **2019**, *2019*, 3831813. [CrossRef]
29. Kurpińska, M.; Kułak, L.; Miruszewski, T.; Byczuk, M. Application of artificial neural networks to predict insulation properties of lightweight concrete. *Appl. Sci.* **2021**, *11*, 10544. [CrossRef]
30. Kursuncu, B.; Gencel, O.; Bayraktar, O.Y.; Shi, J.; Nematzadeh, M.; Kaplan, G. Optimization of foam concrete characteristics using response surface methodology and artificial neural networks. *Constr. Build. Mater.* **2022**, *337*, 127575. [CrossRef]
31. Gencel, O.; Koksal, F.; Sahin, M.; Durgun, M.Y.; Lobland, H.E.H.; Brostow, W. Modeling of thermal conductivity of concrete with vermiculite by using artificial neural Networks approaches. *Exp. Heat Transf.* **2013**, *26*, 360–383. [CrossRef]
32. Lee, J.H.; Lee, J.J.; Cho, B.S. Effective Prediction of Thermal Conductivity of Concrete Using Neural Network Method. *Int. J. Concr. Struct. Mater.* **2012**, *6*, 177–186. [CrossRef]
33. Özel, C.; Topsakal, A. Comparison between ANFIS and ANN for estimation of the thermal conductivity coefficients of construction materials. *Sci. Iran.* **2015**, *22*, 2001–2011.

34. İpek, S.; Yaman, G.Ö.; Kılınç, C. Investigation of thermal conductivity of rubberized concrete as an energy-efficient building material and modeling by artificial intelligence. *Arch. Civ. Mech. Eng.* **2023**, *23*, 168. [CrossRef]
35. Xu, H.; Chang, R.; Pan, M.; Li, H.; Liu, S.; Webber, R.J.; Zuo, J.; Dong, N. Application of Artificial Neural Networks in Construction Management: A Scientometric Review. *Buildings* **2022**, *12*, 952. [CrossRef]
36. Zhu, L.; Dai, J.; Bai, G.; Zhang, F. Study on thermal properties of recycled aggregate concrete and recycled concrete blocks. *Constr. Build. Mater.* **2015**, *94*, 620–628. [CrossRef]
37. Kim, K.-H.; Jeon, S.-E.; Kim, J.-K.; Yang, S. An experimental study on thermal conductivity of concrete. *Cem. Concr. Res.* **2003**, *33*, 363–371. [CrossRef]
38. Vejmelková, E.; Koňáková, D.; Kulovaná, T.; Hubáček, A.; Černý, R. Mechanical and thermal properties of moderate-strength concrete with ceramic powder used as supplementary cementitious material. *Adv. Mat. Res.* **2014**, *1054*, 194–198. [CrossRef]
39. Demirboga, R. Thermal conductivity and compressive strength of concrete incorporation with mineral admixtures. *Build. Environ.* **2007**, *42*, 2467–2471. [CrossRef]
40. Sargam, Y.; Wang, K.; Alleman, J.E. Effects of Modern Concrete Materials on Thermal Conductivity. *J. Mater. Civ. Eng.* **2020**, *32*, 0003026. [CrossRef]
41. Sargam, Y.; Shankaramurthy, B.M.; Wang, K. Characterization of RCAs and their concrete using simple test methods. *J. Sustain. Cem. Based Mater.* **2019**, *9*, 61–77. [CrossRef]
42. Sargam, Y.; Faytarouni, M.; Riding, K.; Wang, K.; Jahren, C.; Shen, J. Predicting thermal performance of a mass concrete foundation—A field monitoring case study. *Case Stud. Constr. Mater.* **2019**, *11*, e00289. [CrossRef]
43. Cavalline, T.L.; Castrodale, R.W.; Freeman, C.; Wall, J. Impact of lightweight aggregate on concrete thermal properties. *ACI Mater. J.* **2017**, *114*, 945–956. [CrossRef]
44. Kurpińska, M.; Karwacki, J.; Maurin, A.; Kin, M. Measurements of thermal conductivity of LWC cement composites using simplified laboratory scale method. *Materials* **2021**, *14*, 1351. [CrossRef]
45. Bayraktar, O.Y.; Kaplan, G.; Gencel, O.; Benli, A.; Sutcu, M. Physico-mechanical, durability and thermal properties of basalt fiber reinforced foamed concrete containing waste marble powder and slag. *Constr. Build. Mater.* **2021**, *288*, 123128. [CrossRef]